Characterization and Extraction of Roads Using Polarimetry Methods in L-Band SAR Images

Paillou Nathan, Laetitia Thirion-Lefevre, Regis Guinvarc'H

CHARACTERIZATION AND EXTRACTION OF ROADS USING POLARIMETRY METHODS IN L-BAND SAR IMAGES

Nathan Paillou , Laetitia Thirion-Lefevre, Régis Guinvarc'h

SONDRA / CentraleSupélec

IGARSS 2021 - 2021 IEEE International Geoscience and Remote Sensing Symposium | 978-1-6654-0369-6/21/$31.00 ©2021 IEEE | DOI: 10.1109/IGARSS47720.2021.9553904

ABSTRACT

Road detection is a well-known subject in optics. For example, it is now possible to perform a road extraction and calculate a travel time using multiple look angles optic data [1]. In SAR, road extraction is not new neither [2, 3], even if it is less developed. When it comes to detection in SAR images, it is most of the time about detecting a small target with high intensity, and if the data set is temporal, the target is punctual and present at few dates. However, it is different here for roads, as they can be thin but are often long, have low radiometry, and are permanent in time. This article shows that it might be possible to characterize roads compared to their environment using temporal methods. A proposition for road extraction based on these road's characterizations is shown, and ideas about improving the extraction are presented.

Index Terms— SAR, Road Extraction, Temporal, Polarimetry, Entropy, Differential Entropy, Intensity

1. INTRODUCTION

The position and the practicability of roads are two important parameters to know, and they may change due to natural events. The detection of roads is a well-known and straightforward subject in optics, but SAR has the advantage that it can be used where optics is ineffective. For instance,in forests, optical wavelength cannot penetrate through the canopy to detect the roads under the trees. It has been shown [4] that to detect them, temporal methods are better than spatial ones as there is no loss of spatial information when filtering the noise. Therefore roads do not disappear in their surrounding. Three different temporal methods are presented in this article to characterize roads compared to their surroundings and extract them. We study here dirt roads, of five meters wide, sometimes in an open area and sometimes bordering forests. Therefore they are hard to detect as they have low radiometry, are narrow compared to the resolution and sometimes covered. These roads are visible using optical data; the objective of this article is to present a methodology for road extraction, not to show the advantage of SAR over optical. First, the three methods will be presented. Then the results obtained to characterize the different Regions of Interest (ROI) used are presented. Finally, roads extractions will be performed and discussed.

Acknowledgement: UAVSAR data courtesy NASA/JPL-Caltech.

2. DATA PRESENTATION

The data used are UAVSAR data provided by the Jet Propulsion Laboratory and collected near Québec, Canada. They are L-band SAR images acquired in PolSAR mode, full-polarized, and with a resolution of 0.6m in azimuth and 1.6m in range. Therefore, in the worst-case, roads are 3 pixels wide. As a consequence, the use of spatial methods will complicate their extraction. The Noise Equivalent Sigma Zero is of -50dB, and the radar is left looking. There are six acquisitions in the temporal stack, obtained in a real close time and by pair. Two acquisitions were acquired on August 5, 2009, two others on August 7, 2009, and the last two were acquired on August 14, 2009. The area studied in this article is inside the white rectangle in Figure 1. The blue arrow symbolizes the flight direction.

A total of 5 Regions of Interest (ROI) have been used, as shown in Figure 2: a ROI of forest in green, one of road in red; one is in orange and is called "open area" which refers to short vegetation without trees; one is a ROI of water (blue), and the last one is black corresponds to shadow.

Fig. 1: Studied area with UAVSAR data, inside the white rectangle near Québec, Canada (Google Earth Image)

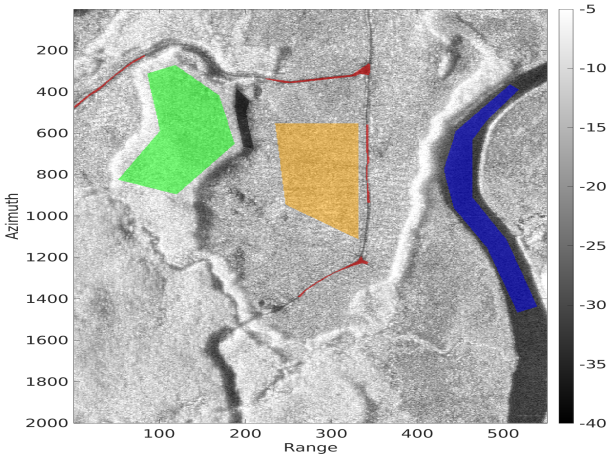

Fig. 2: Masks used over the temporal Intensity for the HH polarization: Forest in green, Road in red, Open Area in orange, Water in blue and, Shadow in black

3. METHODOLOGY

The UAVSAR data used here are calibrated in amplitude and phase and coregistered through time. As we want to realize temporal study, calibration and coregistration are two essential steps to know a pixel's values through time has a physical meaning. Three different methods are used to calculate temporal quantities, and the ability of these quantities to differentiate the 5 ROI will be discussed.

The first method studied is the temporal entropy described in [4, 5], which is based on the spatial entropy of Cloude-Pottier [6]. For a chosen pixel (i,j), a temporal coherency matrix $[T^{Temporal}]$ is calculated as shown in Eq1, averaging N coherency matrices, where N is the number of dates available. These coherency matrices are obtained using the target vector $\underline{k}^n$ described in Eq2, where n denote for the nth acquisition, and S^n_{XY} are the coefficients of the Sinclair Matrix $[S^n]$ of the nth acquisition. The temporal entropy $H^{Temporal}$ is then calculated the same way it is done for the spatial case [6], calculating the eigenvalues of $[T^{Temporal}]$ and the Shannon entropy of these eigenvalues.

$$[T^{Temporal}] = \frac{1}{N}\sum_{n=1}^{N} \underline{k}^n \underline{k}^{n*T} \tag{1}$$

$$\underline{k}^n = \frac{1}{\sqrt{2}}\begin{bmatrix} S^n_{HH} + S^n_{VV} & S^n_{HH} - S^n_{VV} & 2S^n_{HV} \end{bmatrix}^T \tag{2}$$

In [5], a high temporal entropy (0.7) has been obtained for the roads and a low one for the water (0.3), using UAVSAR data. Therefore, the same results are expected to be obtained. Concerning forest and open area ROI, a high temporal entropy (0.85) for the first one and a lower one (0.4) for the second one have been obtained in [4].

The second method is the differential entropy of a Gaussian distribution [7]. It is a measure of relative information, calculated using Eq3, where $[x]$ is a matrix, which columns are variables following a Gaussian distribution, M is the number of variables, and $[C]$ is the covariance matrix of $[x]$.

$$H^{Differential}([x]) = \frac{1}{2}\ln\left((2\pi e)^M det([C])\right) \tag{3}$$

The $[x]$ matrix columns used in this study are composed of the different temporal values of the real or imaginary part of one or more polarizations of the chosen pixel. For example, using only the HH polarization, where S^n_{HH} is the coefficient of the Sinclair Matrix for the HH polarization and the nth acquisition, we have :

$$[x] = \begin{pmatrix} real(S^1_{HH}) & imag(S^1_{HH}) \\ \cdots\cdots & \cdots\cdots \\ \cdots\cdots & \cdots\cdots \\ \cdots\cdots & \cdots\cdots \\ real(S^N_{HH}) & imag(S^N_{HH}) \end{pmatrix} \tag{4}$$

The advantage of differential entropy over temporal entropy is that it is not needed to have all the polarization to work.

The final method presented in this article is the temporal intensity. It is obtained by averaging the intensity for a chosen pixel through time. The case for the VV polarization is presented in Eq5 :

$$\sigma^{Temporal}_{VV} = \frac{1}{N}\sum_{n=1}^{N} {S^n_{VV}}^2 \tag{5}$$

4. RESULTS

The temporal entropy obtained is presented in Figure 3. The results obtained are consistent with the previous section's expectations for the forest, road, and open area ROI. As it is possible to see in Table 1, the road's and forest's temporal entropies are high compared to the open area's temporal entropy. The unexpected value is for the water ROI, as the temporal entropy is high while the result obtained using UAVSAR data in [5] was low over the ocean near San Francisco. However, the water ROI is here from a river and not an ocean, which could explain the difference. Indeed it is possible to see temporal changes over the six acquisitions, which might be due to a water level change. In [5], the temporal entropy for the river in P-band is relatively high too, so this result is not abnormal. For the shadow, the temporal entropy is high, and a distinction can be made compared to the roads. In conclusion, temporal entropy does not allow an easy road extraction, as the statistical values presented for the road ROI are quite similar to the one for the forest.

The second results presented are obtained using only the HH polarization, i.e., x is a 6 by 2 matrix, and using the three

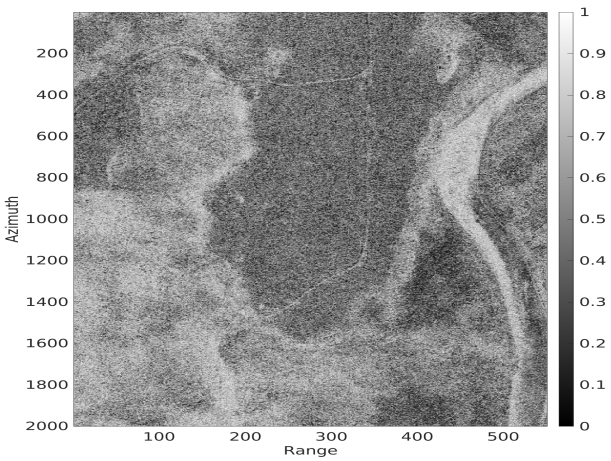

Fig. 3: Temporal Entropy

ROI Name	Forest	Road	Open Area	Water	Shadow
Mean	0.58	0.55	0.42	0.65	0.69
Minimum	0.07	0.09	0.02	0.07	0.18
Maximum	0.97	0.95	0.94	0.99	0.96

Table 1: Statistics for the Temporal Entropy over 5 ROI

polarizations, i.e., x is a 6 by 6 matrix. The results obtained show that using the three polarizations allows reducing the speckle and is, therefore, an advantage to extract roads. Table 2 and Table 3 show that the distribution of the values is also more spread out when using the three polarizations than when using only one polarization, which makes easier the choice of a threshold value to extract roads. The differential entropy allows a road extraction as the road ROI values are significantly different from the forest and open area ROI values. Nevertheless, the road, water, and shadow ROI values are close, and therefore the differentiation is difficult between these 3 areas.

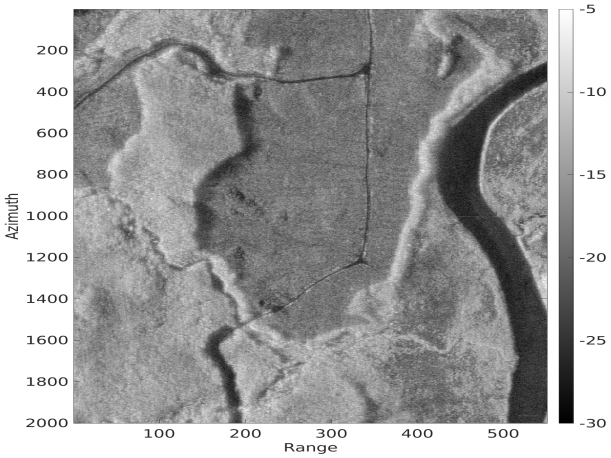

Fig. 4: Differential Entropy using HH, HV, and VV

The final results presented are obtained for the temporal

ROI Name	Forest	Road	Open Area	Water	Shadow
Mean	-0.84	-4.54	-1.83	-5.29	-4.42
Minimum	-4.8	-7.41	-6.12	-8.18	-7.58
Maximum	2.55	-1.44	1.97	-2.24	-1.04
Max-Min	7.35	5.97	8.09	5.94	6.54

Table 2: Statistics for the Differential Entropy HH (5 ROI)

ROI Name	Forest	Road	Open Area	Water	Shadow
Mean	-14.84	-23.87	-18.36	-25.45	-24.03
Minimum	-22.98	-30.15	-26.87	-32.21	-29.98
Maximum	-7.47	-17.71	-10.27	-17.5	-18.25
Max-Min	15.51	12.44	16.6	14.71	11.73

Table 3: Same as Table 2 with HH HV VV

intensity. As for the differential entropy, the temporal intensity allows road extraction as the difference between road ROI and forest and open area ROI is significant, as shown in Table 4. Another point that can help the road extraction is that the two vegetation ROI's temporal intensity is higher for the HH polarization than for the VV polarization, while it is the opposite for the road ROI. However, the distinction between road and shadow is again complicated.

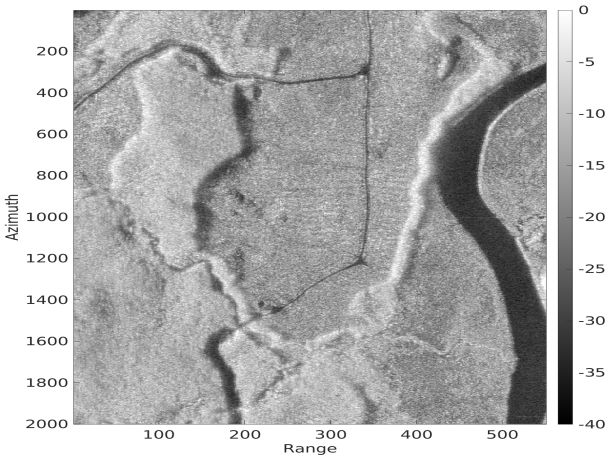

Fig. 5: Temporal Intensity HH polarization in dB

5. ROAD EXTRACTION AND DISCUSSION

In this part, a road extraction is presented using the differential entropy with the three polarizations. A threshold has been set at -23, slightly more than the mean value for the road ROI. The pixels under this threshold have been highlighted in red in Figure 6. The roads are well detected, but also the river and shadows. For the road ROI, 51.7% of the pixel are in red, 96.3% for the water ROI, and 72.1% for the shadow ROI. In terms of Differential Entropy, all these ROIs have similar signatures. We have to find additional characteristics to dis-

ROI Name	Forest	Road	Open Area	Water	Shadow
Mean HH	-10.35	-25.32	-12.81	-30.57	-25.66
Mean HV	-17.57	-31.33	-21.86	-35.17	-32.01
Mean VV	-13.51	-21.81	-15.2	-25.23	-25.84

Table 4: Mean for the Temporal Intensity for the three polarizations over the 5 ROI

criminate them. A first possibility is to use intensity. Indeed, in this study, the intensities of the river are lower than the road ones for all polarizations, as illustrated in Table 4. To correct this, a threshold on the temporal intensity has been set at -30/-34/-28 dB for the HH/HV/VV polarization. The result is presented in Figure 7. It is possible to see that the water is not detected anymore, 2%. However, the shadow is still partially detected, 14.8%, and the road's detection has been lowered, 22.6%.

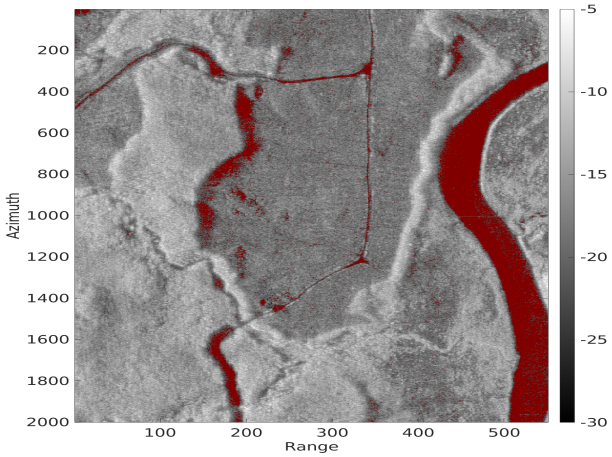

Fig. 6: Road extraction using a threshold at -23 on the Temporal Differential Entropy HH HV VV

In this paper, we proposed to consider the detection of roads, that are small ROIs with low RCS. Temporal methods have been used instead of the usual spatial methods to avoid removing the roads doing a spatial averaging as they are few pixels wide. We proceeded in two steps: first, we used the differential entropy, and then the temporal intensity. For the first step, we observed that the use of the three polarimetric channels improved the results. Then, the second step was needed to differentiate roads from other ROIs with small RCS such as rivers and shadows. Studies still have to be done on the differentiation between roads and shadows, and in particular investigations on the characterization of shadows signatures are conducted.

6. REFERENCES

[1] A. Van Etten, D. Hogan J. Shermeyer, N. Weir, and R. Lewis, "Road network and travel time extraction from multiple look angles with spacenet data," in *2020 IEEE Geoscience and Remote Sensing Symposium*, 2020.

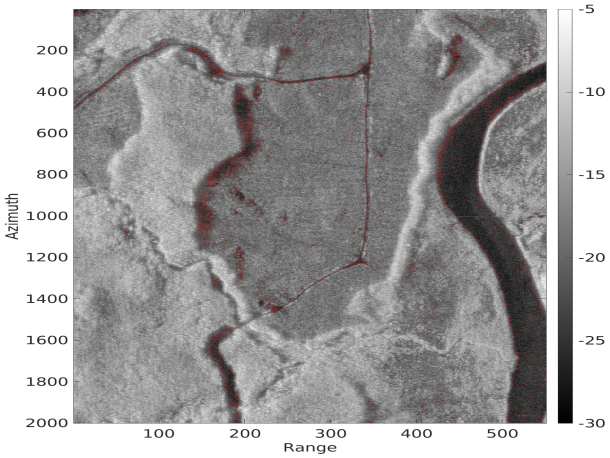

Fig. 7: Road extraction using a threshold at -23 on the Temporal Differential Entropy HH HV VV and at -30/-34/-27dB on the Temporal Intensity HH/HV/VV

[2] C. Fu, Y. Chen, L. Tong, M. Jia, L. Tan, and X. Ji, "Road damage information extraction using high-resolution SAR imagery," in *2014 IEEE Geoscience and Remote Sensing Symposium*, 2014, pp. 1836–1838.

[3] C. He, B. Shi, Y. Zhang, X. Xu, and M. Liao, "Road extraction for SAR imagery based on the combination of beamlet and a selected kernel," in *2014 IEEE Geoscience and Remote Sensing Symposium*, 2014, pp. 2257–2260.

[4] N. Paillou, L. Thirion-Lefevre, and R. Guinvarc'h, "Interest of temporal methods over spatial methods in order to detect small target," in *2020 IEEE Geoscience and Remote Sensing Symposium*, 2020.

[5] F. Weissgerber, E. Colin-Koeniguer, N. Trouvé, and J.-M. Nicolas, "A temporal estimation of entropy and its comparison with spatial estimations on PolSAR images," in *IEEE Journal of Selected Topics in Applied Earth Observations and Remote Sensing*, Aug 2016, vol. 9, pp. 3809–3820.

[6] E. Pottier and S. R. Cloude, "Unsupervized classification of full polarimetric SAR data and feature vectors identification using radar target decomposition theorems and entropy analysis," in *1995 International Geoscience and Remote Sensing Symposium*, July 1995, vol. 3, pp. 2247–2249.

[7] M. F. Huber, T. Bailey, H. Durrant-Whyte, and U. D. Hanebeck, "On entropy approximation for gaussian mixture random vectors," in *2008 IEEE International Conference on Multisensor Fusion and Integration for Intelligent Systems*, 2008, pp. 181–188.